United States Department of Agriculture
Natural Resource Conservation Service
160 East 7th Street
Chester, PA 19013-6092
610-490-6042

Subject: Geophysical field assistance **Date:** June 5 1995

To: Warren Henderson
State Soil Scientist
USDA - NRCS
P. O. Box 141510
Gainesville, Florida
32614-1510

Purpose:
To provide ground-penetrating radar (GPR) and electromagnetic induction (EM) soils field assistance and training. In addition, a preliminary study comparing the effectiveness of GPR and EM techniques in areas of karst was conducted near Archer, Florida.

Participants:
Jeff Allen, Area Resource Soil Scientist, NRCS, Marianna, FL
Gary Bowden, Engineer, Okaloosa County Roads Department, Crestview, FL
Kevin Brown, Area Conservationist, NRCS, Marianna, FL
Mary Collins, Professor of Soil, Univ. of Florida, Gainesville, FL
Eddie Cummings, Soil Specialist (GPR), NRCS, Lake City, FL
James Doolittle, Research Soil Scientist, NRCS, Chester, PA
Art Hornsby, Professor of Soil Physics, Univ. of Florida, Gainesville, FL
Ron Kuhl, Soil Scientist, Soil Environmental Services, Gainesville, FL
James Kurtz, Electronic Comm. Lab., Univ. of Florida, Gainesville, FL
Doug Lewis, Soil Specialist (GPR), NRCS, Sebring, FL
Raymond Tedder, Engineer, Okaloosa County Roads Department, Crestview, FL
Andrew Williams, Soil Specialist (GPR), NRCS, Lake City, FL
Darryl Williams, District Conservationist, Crestview, FL

Activities:
On 1 May, 1995, I completed my travel to Crestview, Florida, with Eddie Cummings. On the morning of 2 May, GPR surveys were completed along several sections of roadways and bridge decks in Okalossa County with the Okaloosa County Roads Department. During the afternoon of 2 May, we travelled to Gainesville, Florida. On 3 May a comparative study of two geophysical techniques was conducted near Archer, Florida. The purpose of this study was to assess depths to limestone bedrock with both GPR and EM techniques. During both of these field studies, time was spent familiarizing soil scientists with the operation of the SIR System-2 radar unit. On 4 and 5 May, I returned to Chester, Pennsylvania.

Equipment:
The radar units used during this period of field investigations were the Subsurface Interface Radar (SIR) System-2 and System-3 manufactured by Geophysical Survey Systems, Inc. (GSSI). The recently developed System-2 unit is highly portable and can be fitted into a backpack. The SIR

System-2 consists of a digital control unit (DC-2) with keypad, VGA video screen, and connector panel. The SIR-3 (Florida's unit) consists of the Model PR8300 profiling recorder and a power distribution unit. The systems were powered by 12-volt vehicular battery. The model 3110 (120 mHz) antenna was used in this investigation.

The electromagnetic induction meters were the EM38 and EM31, manufactured by GEONICS Limited. The observation depth of an EM meter is dependent upon intercoil spacing, transmission frequency, and coil orientation relative to the ground surface. The EM38 meter has a fixed intercoil spacing of 1.0 m. It operates at a frequency of 13.2 kHz. The EM38 meter has effective observation depths of about 0.75 and 1.5 m in the horizontal and vertical dipole orientations, respectively. The EM31 meter has a fixed intercoil spacing of 3.66 m. It operates at a frequency of 9.8 kHz. The EM31 meter has effective observation depths of about 3 and 6 m in the horizontal and vertical dipole orientations, respectively. Measurements of conductivity are expressed as milliSiemens per meter (mS/m).

Discussion:

GPR surveys of roadways and bridge decks in Okalossa County
Both the SIR System-2 and System-3 units with 120 mHz antennas were used in these investigations. Both systems provided comparable results. The ability of the SIR System-2 to store and process radar data was beneficial to field operations. In some areas, playing back and printing the recorded and processed data enhanced the radar imagery and improved interpretations.

Ground-penetrating radar provided detailed subsurface information to highway engineers interested in characterizing and assessing the extent of slumping and solution features beneath roadways. This is a good application for GPR. The most appropriate antennas for this application operate at center frequencies of 80 or 120 mHz.

Comparative Study of EM and GPR Techniques
Wilson (1995) noted that for every observable sinkhole, there exist a greater number of buried sinkholes and dissolution openings which lack surface expressions. Buried sinkholes are former sinkholes that have been filled with sediment. In terms of risk assessment, buried sinkholes are considered unstable and vulnerable to renewed subsidence (Wilson, 1995). In areas of karst and for a particular land use, if the expected economic loss or the potential for groundwater contamination is considered high, mitigation involving comprehensive and systematic sampling and the use of high geophysical tool is often desirable and cost effective.

Ground penetrating radar techniques were first used by the Soil Conservation Service in Florida. Ground-penetrating radar is best suited for shallow (3 to 10 meters) investigations in electrically resistive mediums (i.e. dry, coarse-textured soils). The extensive occurrence of coarse-textured soil materials in Florida provides a most favorable environment for the use of GPR. In Florida, GPR has been used to detect and delineate shallow karst features (Ballard, 1983; Barr, 1993; Collins et al., 1990; Collins et al., 1994; Filler and Kuo, 1989; Hearns, 1987; Puckett et al., 1990; and Wilson, 1995). The use of GPR in other karst

areas of the United States has been more restrictive and less effective (Carter et al., 1986, Mellett and Maccarillo, 1995).

In some areas of finer-textured soil materials, electromagnetic induction (EM) methods has been used to determine the depths to bedrock (Palacky and Stephens, 1990; Zalasiewicz et al., 1985) and to locate water-bearing fracture zones in bedrock (McNeill, 1991; Olayinka, 1990). These studies have documented that this noninvasive technique is relatively inexpensive and fast, can provide comprehensive coverage of sites and the large number of observations needed for site characterization and assessments, and is applicable over broad areas and soils. Maps prepared from correctly interpreted EM data provide the basis for assessing site conditions and planning further investigations.

Electromagnetic induction techniques have been used in areas of karst (Canace and Dalton, 1984; Pazuniak, 1989; Robinson-Poteet, 1989; Rumbens, 1990). Interpretations of EM data have enabled the delineation of subsurface voids, channels, and zones of higher permeability such as fractures and karstified areas within carbonate bedrock. Typically, the shape and pattern of the discontinuity or subsurface anomaly have been used to identify the solution feature.

Study Site:
The study site was located in a pasture near Archer, Florida. The survey grid was arranged to include a portion of a sinkhole. Relief was about 5.5 feet. Figure 1 is a three-dimensional surface net of the study site. The contour interval is 0.5 feet.

The site was in an area of Candler-Apopka complex, 0 to 5 percent slopes. Candler and Apopka soils are members of the hyperthermic, uncoated Typic Quartzipsamments and the loamy, siliceous, hyperthermic Grossarenic Paleudults families, respectively. Included with these soils in mapping were small areas of Jonesville and Pedro soils. Jonesville and Pedro soils are members of the loamy, siliceous, hyperthermic Arenic Hapludalfs and the fine-loamy, siliceous, hyperthermic, shallow Typic Hapludalfs families, respectively. Jonesville and Pedro soils are moderately deep and shallow over limestone bedrock.

Field Methods:
A 100 by 175 foot grid (0.40 acre) was established across the site. The grid interval was 25 feet. This interval provided 40 grid intersections or observation sites. At each grid intersection, the relative elevation of the surface was determined with a level and stadia rod. Elevations were not tied to an elevation benchmark; the lowest recorded grid intersection was recorded as the 80 foot datum.

At each grid intersection, measurements were taken with an EM38 and an EM31 meter. Measurements were taken with each meter placed on the ground surface in both the horizontal and vertical dipole orientations.

A radar survey of the site was completed using the SIR System-2 radar and a 120 mHz antenna. Scanning times of 120 and 200 nanoseconds were used. Survey procedure involves towing the 120 mHz antenna along a grid line at an average speed of about 0.6 miles h^{-1}. The operator attempted to maintain a constant speed of advance along each grid line and to record the position of each grid intersect as the antenna drew abreast of the

survey flags. Traverses were completed in a north-south direction only. The cumulative length of traverses completed with the GPR was 875 feet.

To help summarize the results of this survey, the software program SURFER for Windows was used to construct two- and three-dimensional simulations. In several simulations, to help emphasize the spatial distribution of apparent conductivity values, colors and filled contour lines were used. These plots represent the spatial distribution of apparent conductivity values over a specified observation depth. Other than showing trends in values of apparent conductivity (i.e. zones of higher or lower electrical conductivity), no significance should be attached to the colors themselves.

Results:

GPR Survey

Based on the depths to the sand/limestone or the sand/clay interface observed in auger borings at four observation points and the corresponding time intervals to these interfaces on radar profiles, the velocity of signal propagation was estimated to be 0.090336 ft/ns. The dielectric constant was 11. The velocity of propagation was used to scale the radar profiles and to determine the thickness of the surficial sand deposits.

Because of a strong surface reflection and the limited resolution of the 120 mHz antenna, interfaces occurring within the upper 16 inches of the soil profile were difficult to resolve. Using a higher frequency antenna would help to resolve shallow interfaces.

Within the study site, GPR provided highly interpretable images of the interface separating the sandy surface layers from the underlying limestone bedrock or the medium-textured argillic horizon. In general, with GPR, the depth of observation is restricted to the upper part of the argillic horizon. Ballard (1993), Barr (1993), and Collins and others (1994) noted that in areas where the limestone bedrock was capped by a medium- to fine-textured overburden, the radar signal was rapidly attenuated by and did not penetrate this relatively conductive layer. The depth of observation is therefore dependent upon the depth and electrical conductivity of the morphological Bt horizons. Fortunately, many buried, sand-filled sinkholes have been identified by the subsurface topography of the clay layers which have subsided into and follows the shape of these dissolution features (Collins et al., 1990).

Figure 2 is a processed radar profile from the study site. This profile has been processed through the RADAN software package. Processing was limited to signal stacking, horizontal scaling, color transform and table customizing, and annotations. The horizontal and vertical scales are in feet and measure distances along the transect line and depths, respectively.

In Figure 2, the upper-most, continuous interface represents the boundary separating the sandy surface layers from the underlying argillic horizon or limestone bedrock. This interface has been highlighted by a dark line. On unprocessed radar profiles, this interface often appears as two or three, dark, sub-parallel bands. In Figure 2, color transformation and customization have been used to reduce signal amplitudes and background noise (continuous band located immediately below "B"). As a consequence, the sand/clay or sand/limestone interface appears as a lone

intermittent band. In Figure 2, this interface ranges in depth from about 1.8 to 10.7 feet.

Because of their similar dielectric properties and reflection coefficients, the limestone bedrock could not be distinguished from the argillic horizon. Exceptionally high rates of attenuation in the medium-textured argillic horizon limited signal penetration to the upper part of this layer. Rates of signal attenuation were substantially less in portions of the profile where surface layers were thicker and/or the argillic horizon was thin or absence. Depths of observation were greater in these areas. As a consequence of these differences in the rates of signal attenuation and the depths of observation, in Figure 2, it was presumed that the sandy surface layers were underlain by an argillic horizon of varying thickness between observation points 0 and 125, and by limestone bedrock and/or a very thin argillic horizon between observation points 150 and 175. The multiple dark bands to the right of "A" in the center of the sinkhole were presumed to represent dissolution or collapsed features within the limestone bedrock. In Figure 2, a rock fragment or limestone pinnacle is apparent to the left of "C."

Figure 3 is a three dimensional surface net diagram of the soil and the underlying clay/limestone surface. These simulations were compiled from elevation and GPR data. In general, the topography of the underlying clay/limestone surface resembles the topography of the soil surface, but it is more irregular and has greater relief. The surficial sand deposits appear to have blanketed and subdued the expression of an undulating clay/limestone surface and the buried sinkhole.

EM Survey

Interpretations of the EM data are based on the identification of spatial patterns within the data set. Figures 4 contains two-dimensional plots of the EM data collected with the EM38 and the EM31 meters in the horizontal and vertical dipole orientations. These plots are based on measurements collected from 40 observation points. In each plot, the interval is 1 mS/m.

Comparing the plots appearing in Figure 4, values of apparent conductivity, as a rule, increase with increasing observation depth (responses of the EM38 meter were less than those of the EM31 meter, and, for each meter, responses in the horizontal dipole orientation were typically less than those in vertical dipole orientation). The lower EM responses at shallower observation depths were attributed to the low clay and moisture contents of the sandy surface layers. The higher EM responses with increased observation depths were attributed to the greater moisture, clay, and soluble salt contents of the underlying argillic horizon and limestone bedrock.

Electromagnetic induction is an imperfect tool and is not equally suitable for use in all soil investigations. Generally, the use of EM techniques has been most successful in areas where subsurface properties are reasonably homogeneous, the effects of one factor (clay, water, or salt content) dominates over the other factors, and variations in EM response can be related to changes in the dominant factor (Cook et al., 1992). In such areas, information is gathered on the dominant factor, and assumptions are made concerning the behavior of the other factors (Cook et al., 1989).

At the Archer site, subsurface properties were relatively variable. The site was characterized as consisting of a relatively thin mantle of sands overlying more conductive materials of the Hawthorne Formation and the Crystal River limestone. These materials were of variable thickness. In some areas, the medium-textured materials of the Hawthorne Formation was absence.

At the Archer site, three factors (clay, moisture, and salt contents) varied making it difficult to attribute variation in the EM response to the depth to clay or limestone bedrock alone. At the Archer site and for much of Florida, the use of EM techniques to determine the thickness of sand deposits, the depth to clay and limestone, and the location of solution features and buried sinkholes is considered less effective than GPR techniques. Compare with GPR, EM is less depth restricted, but provides poorer resolution of subsurface features.

Within the site, the range of EM responses was exceedingly low (3.5 to 13.6 mS/m). A fairly broad zone of noticeably lower EM responses was evident in the southern (upper section of plots) and central portions of the study site. It was inferred from these low responses that the surface layers were thicker and the depths to the more conductive, argillic horizon or limestone bedrock were greater in these portions of the study site. Electromagnetic responses were generally higher in the northern portion of the study site. These higher response were believed to reflect shallower depths to the argillic horizon or the limestone bedrock.

Basic statistics for the EM measurements collected at 40 observation points within the study site are displayed in Table 1. The depth response of the EM meters conformed with the basic conceptual model for the site. This model predicted that EM responses should increase with increasing depths of observation.

Table 1
Archer Study Site
(all values are in mS/m)

				Quartiles			
Meter	Orientation	Minimum	Maximum	1st	Median	3rd	Average
EM38	Horizontal	4.0	11.5	6.5	7.5	8.0	7.5
EM38	Vertical	3.5	11.5	6.0	6.5	7.5	6.7
EM31	Horizontal	6.0	13.5	8.9	9.7	10.5	9.8
EM31	Vertical	6.5	13.0	7.8	8.7	9.5	9.0

Measurements of the thickness of the surface layer (measured with a tape and a bucket auger) were compared with EM responses obtained at the same observation points. The thickness of sands measured at these four observation points ranged from 24 to 70 inches. Admittedly, the number of ground-truth observations was exceedingly small. This study could have been improved using a large number of observation points for correlation. However, the purposes of the survey were satisfied by this small number of observations.

Tables 2 shows the relationship that existed between the observed thickness of the sandy surface layers and electromagnetic responses collected with the EM38 and EM31 meters. As the observed depths were

well beyond the observation depth of the EM38 meter in the horizontal dipole orientation (0 to 30 inches), no analysis was performed on this data set. The highest correlation was were found between the thickness of sandy surface layers and the responses of the EM38 meter in the vertical dipole orientation.

Table 2
Relationship Among EM Measurements and Thickness of Sandy Surface Layers

Meter and Orientation	r^2
EM38 Meter (Vertical Dipole Orientation)	0.714285
EM31 Meter (Horizontal Dipole Orientation)	0.111111
EM31 Meter (Vertical Dipole Orientation)	0.090909

Data collected with the EM38 meter in the vertical dipole orientations were used to develop the following predictive regression equation:

$$D = 129.1428 + (-26.285 * EM38V) \quad [1]$$

where "D" is depth to the argillic horizon or the limestone bedrock (inches) and "EM38V" is the apparent conductivity (mS/m) measured by the EM38 meter in the vertical dipole orientation. Equation [1] was used to estimate the thickness of sandy surface layers at each grid intersections

Figure 5 is a three dimensional surface net diagram of the soil and the underlying clay/limestone surfaces. These simulations were produced from the elevation data, predictive Equation [1] and the EM measurements. In Figure 5, the topography of the clay/limestone surface is remarkably similar to the plot of the same surface generated from the GPR data (Figure 3). In both plots, the location of the buried sinkhole is in the same general portion of the study site. Sections shallower to bedrock and/or argillic horizons also appear within similar areas of the site. The topography of the underlying clay/limestone surface as predicted from the EM measurements and equation [1] resembles the topography of the soil surface, but it is slightly more irregular and has greater relief. The surficial sand deposits appear to have blanketed and subdued the expression of an undulating clay/limestone surface and the buried sinkhole.

In Figure 6, two-dimensional plots simulate the thickness of surficial sand deposits as predicted from Equation [1] and the EM measurements, and from the scaled radar imagery. The predicted and scaled depths and general spatial patterns are remarkably similar in both plots.

The average thickness of the surficial sand deposits as scaled from the radar imagery was 5.10 feet, with a range of 1.58 to 11.06 feet. The average thickness of the surficial sand deposits as predicted from Equation [1] and the EM data was 5.08 feet, with a range of 1.29 to 6.38 feet. Based on radar measurements, sand deposits were shallow (<20 inch) at 5 percent, moderately deep (20 to 40 inch) at 17 percent, deep (40 to 60 inch) at 20 percent, and very deep (>60 inch) at 58 percent of the observation sites. Based on EM measurements and Equation [1], sand deposits were shallow (<20 inch) at 3 percent, moderately deep (20 to 40 inch) at 15 percent, deep (40 to 60 inch) at 17 percent, and very deep (>60 inch) at 65 percent of the observation sites.

Results:

1. A copy of a video tape covering the general theory of GPR, and the use and operation of the SIR System-2 radar unit was given to Andrew Williams. This video will be shared among the radar operators in Florida. The field trip provided Doug Lewis, Eddie Cummings, and Andrew Williams with an opportunity to become familiar with the operation of the SIR System-2 radar unit.

The SIR System-2 radar unit is highly portable and is suitable for surveying relatively inaccessible and wooded areas in Florida.

2. In Okaloosa County, GPR provided detailed subsurface information to highway engineers interested in characterizing and assessing the extent of slumping and solution features beneath roadways. With a suitable antenna (80 or 120 mHz), GPR is a most appropriate tool for this application.

3. The study at the Archer demonstrated that both EM and GPR techniques can be used to predict the thickness of surficial sand deposits, depths to contrasting materials, and simulate the subsurface topography of layers of contrasting materials. At the scale of mapping, neither technique could distinguish the argillic horizon from the limestone bedrock. The surface layer/argillic horizon and the surface layer/limestone bedrock interfaces provided distinct subsurface reflections and could be distinguished on the radar profiles. However, the thickness of argillic or its boundary with the underlying bedrock could not be differentiated. The variable depth and thickness of the argillic horizon and limestone bedrock made it difficult to attribute variation in the EM response to the depth to clay or limestone bedrock alone. This reduced the reliability of predictive equations developed from EM and auger data. At this site, though both geophysical tools produced similar results, the use of GPR techniques is more appropriate.

It was a pleasure to work with members of your fine staff.

With kind regards.

James A. Doolittle
Research Soil Scientist

cc:
J. Culver, Assistant Director, NSSC, NRCS, Lincoln. NE
E. Cummings, NRCS, Route 10, Box 405N, Lake City, FL 32055
T. Glasgow, State Conservationist, NRCS, Gainesville, FL
C. Holzhey, Assistant Director, NSSC, NRCS, Lincoln, NE
D. Lewis, NRCS, 1251 US 27 South, Sebring, FL 33872
A. Williams, NRCS, 5505 Stewart St., Milton, FL 32570

REFERENCES:

Ballard, R. F. Jr. 1983. Cavity detection and delineation research. Report No. 5: Electromagnetic (radar) techniques applied to cavity detection. U.S. Army Corps of Engineers, Waterways Experiment Station, Vicksburg, Mississippi. Tech. Report GL-83-1. pp. 90.

Barr, G. L. 1993. Application of ground-penetrating radar methods in determining hydrogeologic conditions in a karst area, west-central Florida. USGS Water Resources Investigation Report 92-4141. pp. 26.

Canace, R. and R. Dalton. 1984. A geological survey's cooperative approach to analyzing and remedying a sinkhole related disaster in an urban environment. pp. 342-348. IN: Proceedings of the First Multidisciplinary Conference on Sinkholes. Orlando, Florida. 15 to 17 October 1984.

Carter, T. G., M. L. J. Mahner, A. P. Annan, and J. A. Richard. Specialized investigation techniques for defining karstic cavities. In: Proceedings of the Environmental Problems in Karst Terranes and their Solutions Conference. National Water Well Association. Dublin, Ohio. p. 345-367.

Collins M. E., W. E Puckett, G. W. Schellentrager, and N. A. Yust. 1990. Using GPR for micro-analyses of soils and karst features on the Chiefland Limestone Plain in Florida. Geoderma 47:159-170.

Collins, M. E., M. Crum, and P. Hanninen. 1994. Using ground-penetrating radar to investigate subsurface karst landscape in north-central Florida. Geoderma 61:1-15.

Cook, P. G., M. W. Hughes, G. R. Walker, and G. B. Allison. 1989. The calibration of frequency-domain electromagnetic induction meters and their possible use in recharge studies. Journal of Hydrology 107:251-265.

Cook, P. G. and G. R. Walker. 1992. Depth profiles of electrical conductivity from linear combinations of electromagnetic induction measurements. Soil Sci. Soc. Am. J. 56:1015-1022.

Filler, D. M. and S. S.. Kuo. 1989. Subsurface cavity exploration using non-destructive geophysical methods. Proceedings of the Third National Outdoor Action Conference on Aquifer Restoration. Groundwater monitoring and geophysical methods. National Water Wells Association, Dublin, Ohio. p. 827-840.

Hearns, D. J. 1987. The application of ground-penetrating radar to geologic investigations in karst terrains. M. Sc. thesis. University of Florida, Gainesville, Fl. pp. 107.

McNeill, J. D. 1991. Advance in electromagnetic methods for groundwater studies. Geoexplorations 27:65-80.

Mellett, J. S. and B. J. Maccarillo. 1995. A model for sinkhole formation on interstate and limited access highways, with suggestions on remediation. p. 335-339. IN: Beck, B. F. (ed.) Karst GeoHazards. A. A. Balkema, Rotterdam.

Olayinka, A. I. 1990. Electromagnetic profiling for groundwater in Precambrian basement complex areas of Nigeria. Nordic Hydrology 21:205-216.

Palacky, G. J. and L. E. Stephens. 1990. Mapping of Quaternary sediments in northeastern Ontario using ground electromagnetic methods. Geophysics 55:1596-1604.

Pazuniak, B. L. 1989. Subsurface investigation response to sinkhole activity at an eastern Pennsylvania site. pp. 263-269. IN: Proceedings of the 3rd Multidisciplinary Conference on Sinkholes. St. Petersburg Beach, Florida. 2 to 4 October 1989.

Puckett, W. E., M. E. Collins, and G. W. Schellentrager. 1990 Design of soil map units on a karst area in west central Florida. Soil Science Soc. Am. J., 54:1068-1073.

Robinson-Poteet, D. 1989. Using terrain conductivity to detect subsurface voids and caves in a limestone formation. pp. 271-279. IN: Proceedings of the 3rd Multidisciplinary Conference on Sinkholes. St. Petersburg Beach, Florida. 2 to 4 October 1989.

Rumbens, A. J. 1990. Detection of cavities in karstic terrain: road subsidence - Snowy Mountains Highway near Yarrangobilly, State of new South Wales - Australia. Exploration Geophysics 21:121-24.

Wilson, W. L. 1995. Sinkhole and buried sinkhole densities and new sinkhole frequencies in karsts of northwest Peninsular Florida. p. 79-91 IN: Beck, B. F. (ed.) Karst GeoHazards. A. A. Balkema, Rotterdam.

Zalasiewicz, J. A., S. J. Mathers, and J. D. Cornwell. 1985. The application of ground conductivity measurements to geological mapping. Q. J. English Geol. London 18:139-148.

RELATIVE TOPOGRAPHY

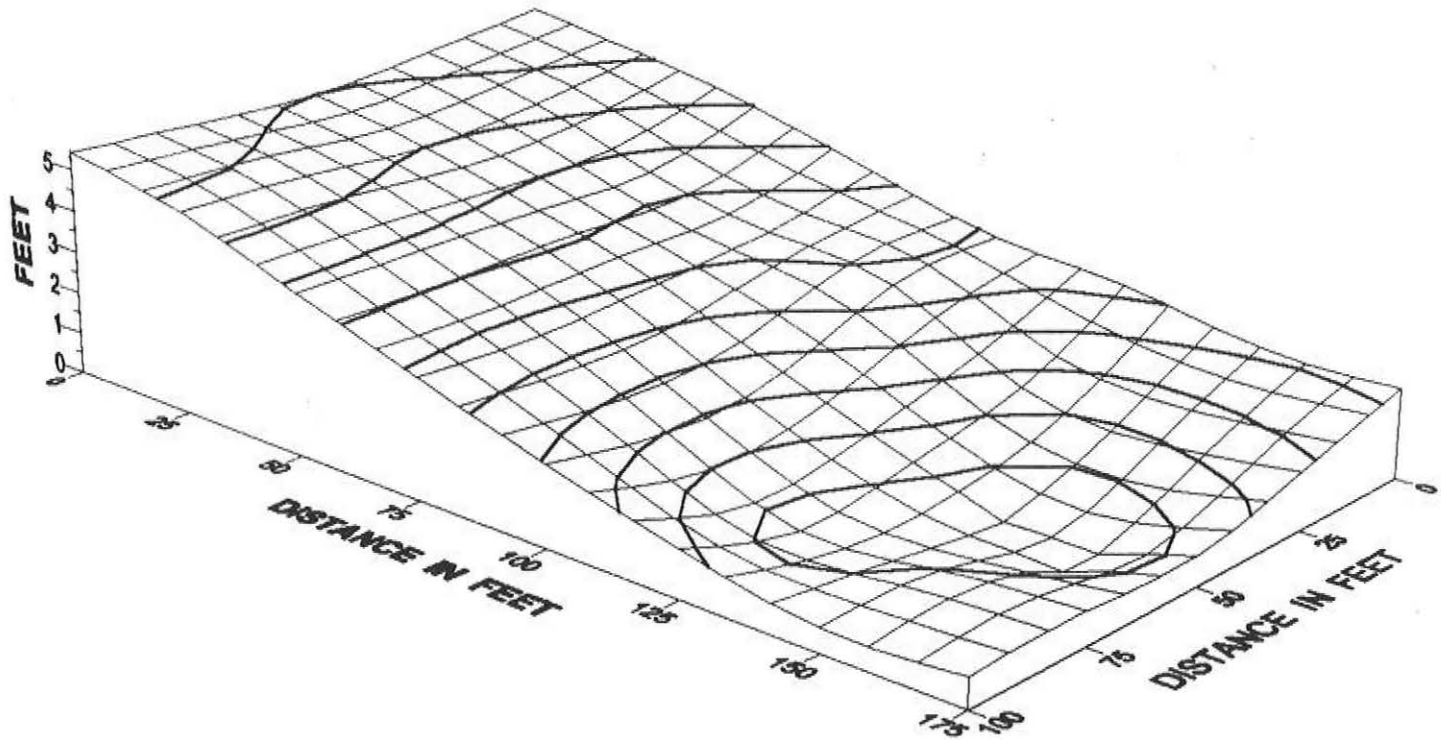

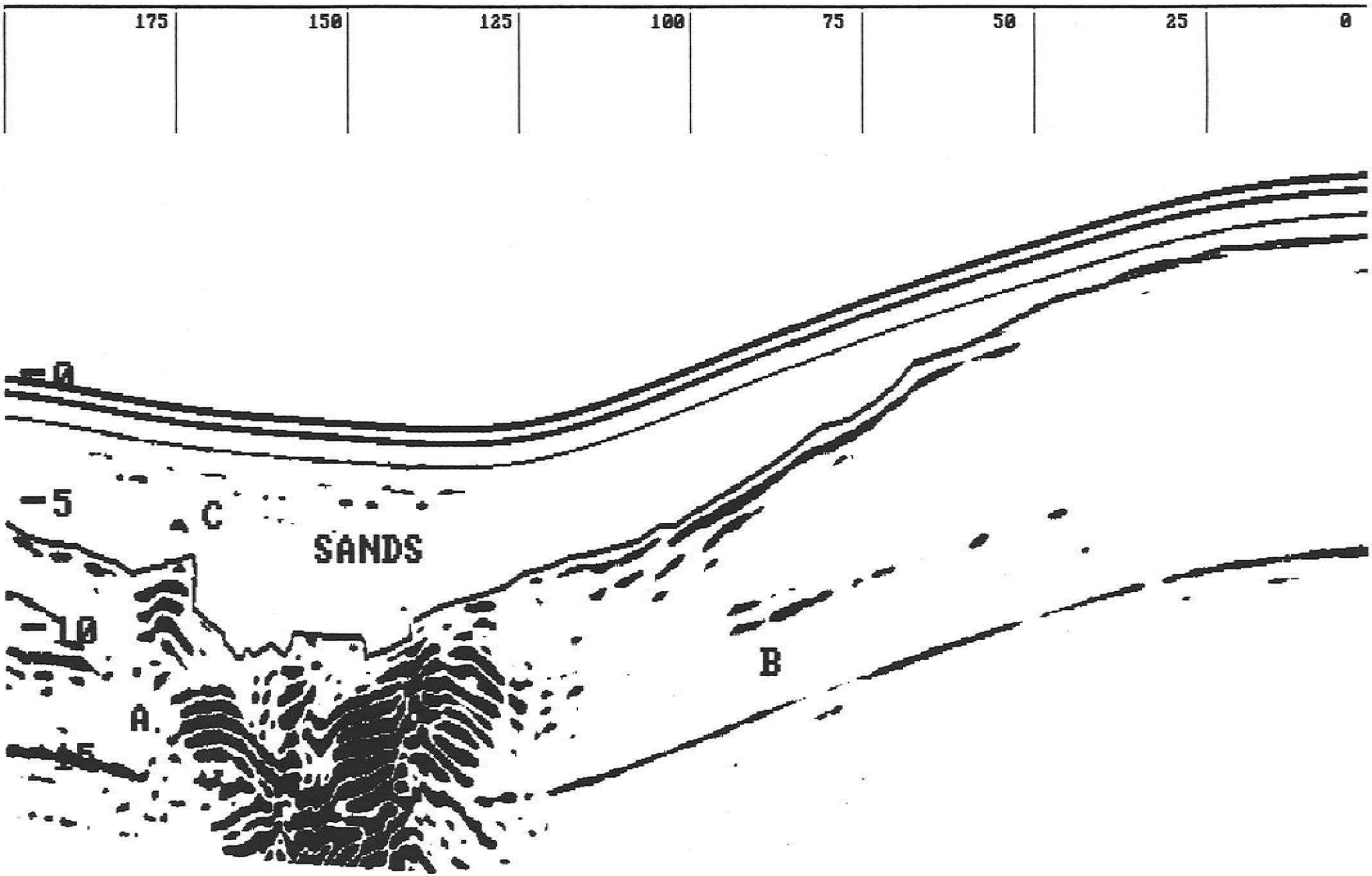
175
150
125
100
75
50
25
0
-0
-5
-10
-15
C
SANDS
A
B

RELATIVE TOPOGRAPHY
OF THE
SOIL AND BEDROCK SURFACES

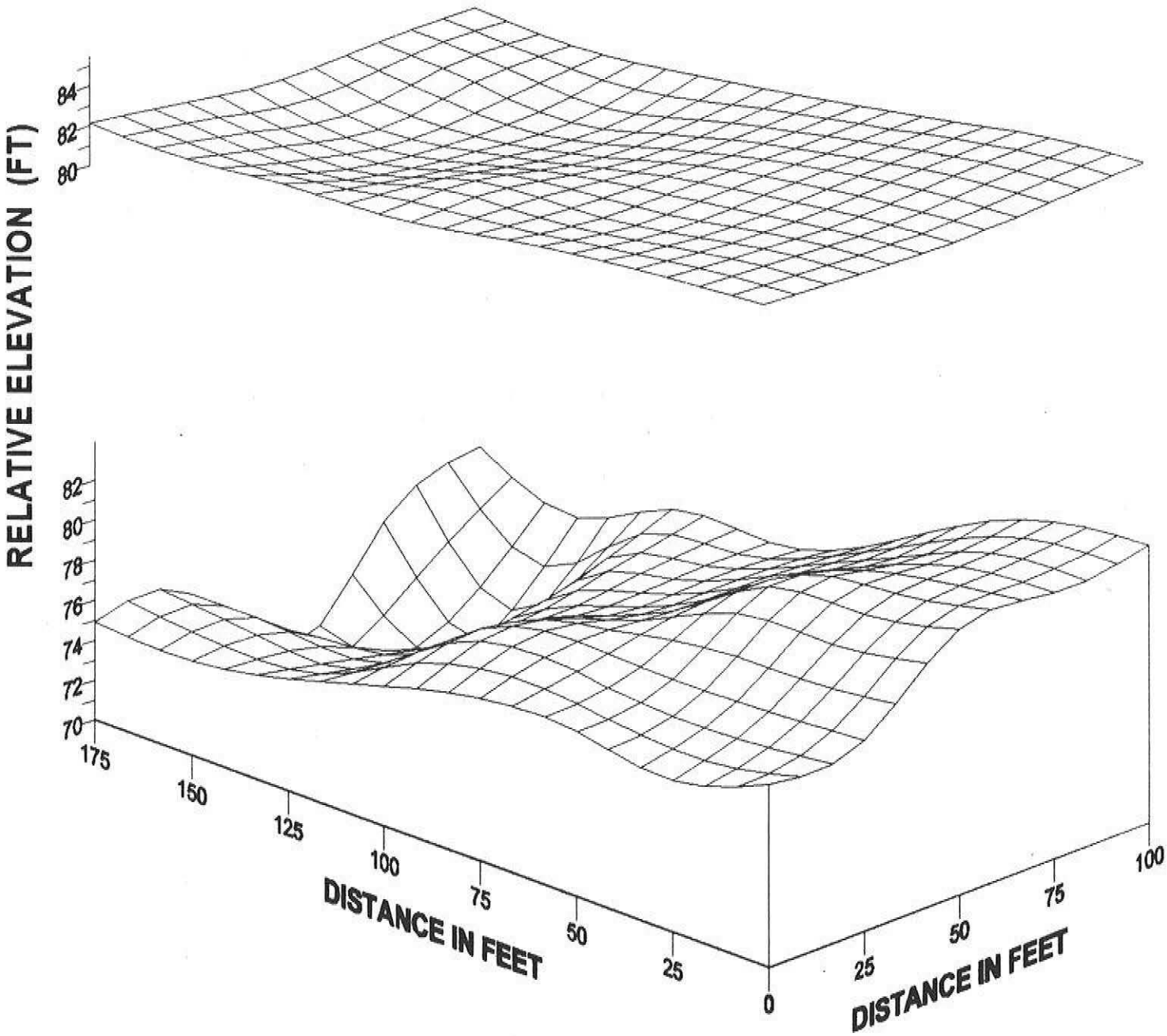

HORIZONTAL DIPOLE ORIENTATION

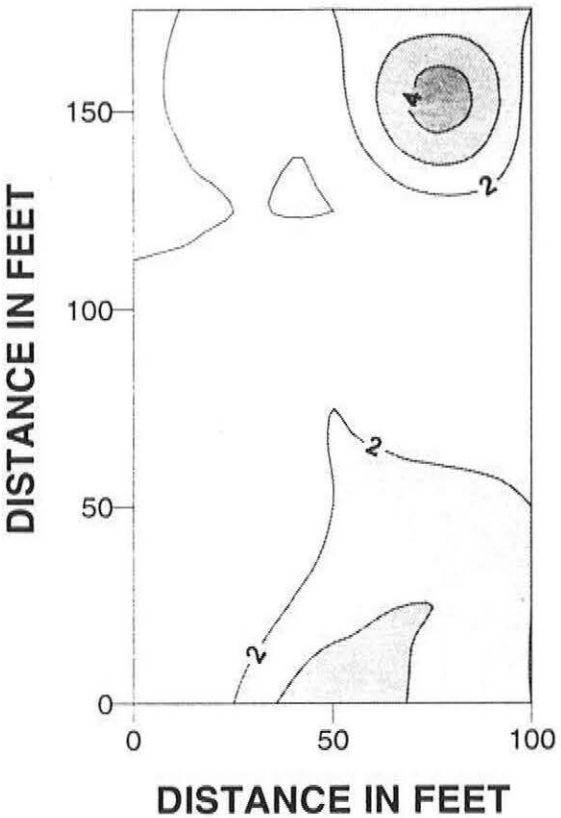

VERTICAL DIPOLE ORIENTATION

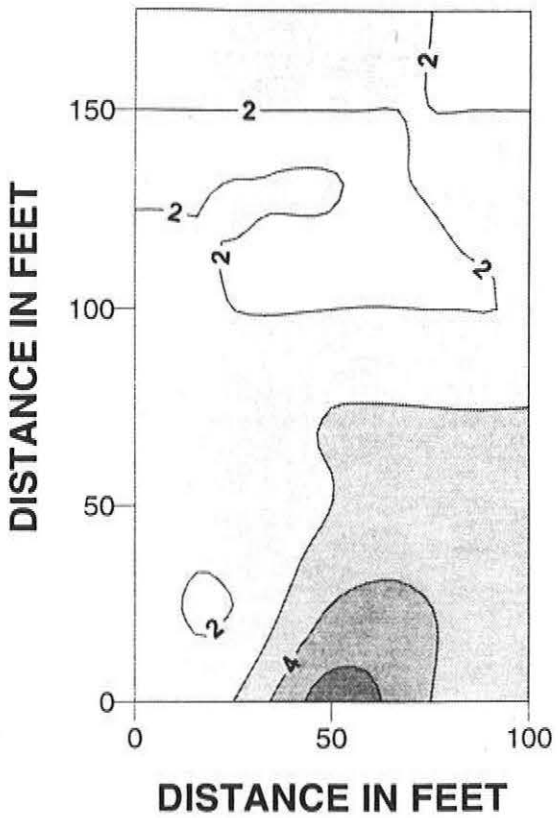

EM31 METER
HORIZONTAL DIPOLE ORIENTATION

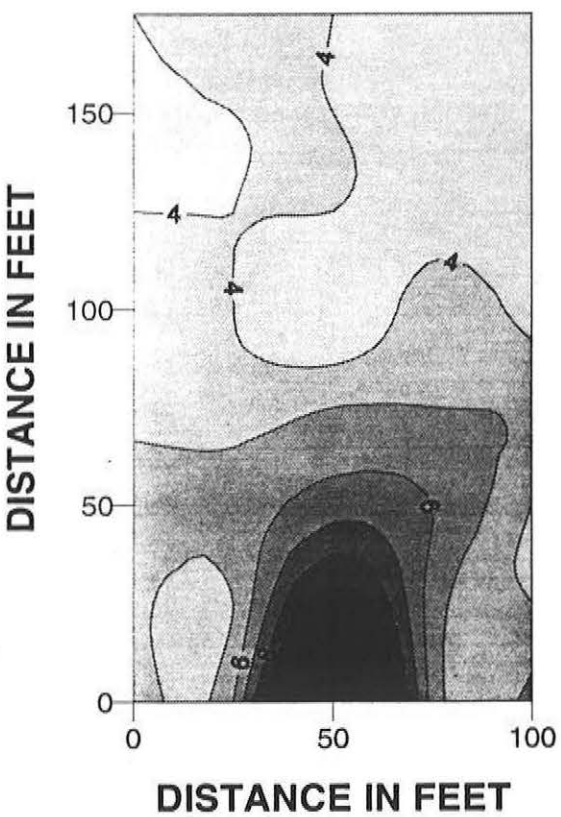

EM31 METER
VERTICAL DIPOLE ORIENTATION

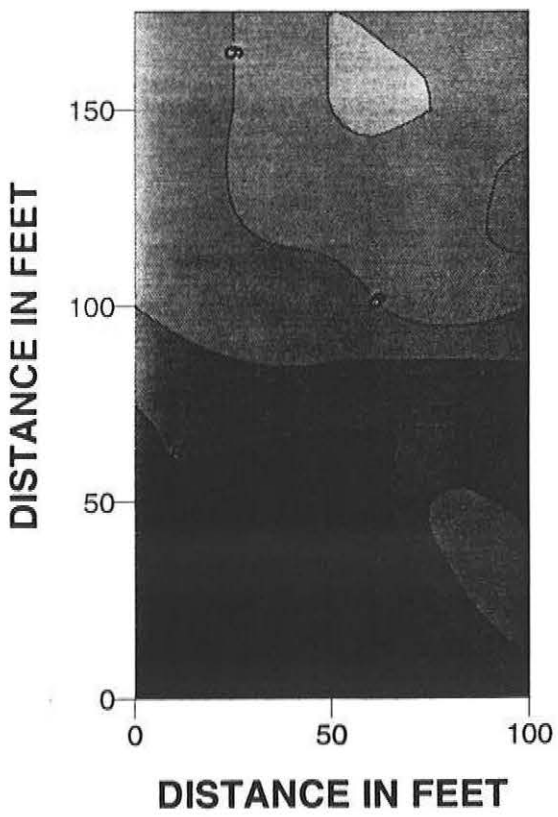

RELATIVE TOPOGRAPHY
OF THE
SOIL AND BEDROCK SURFACES

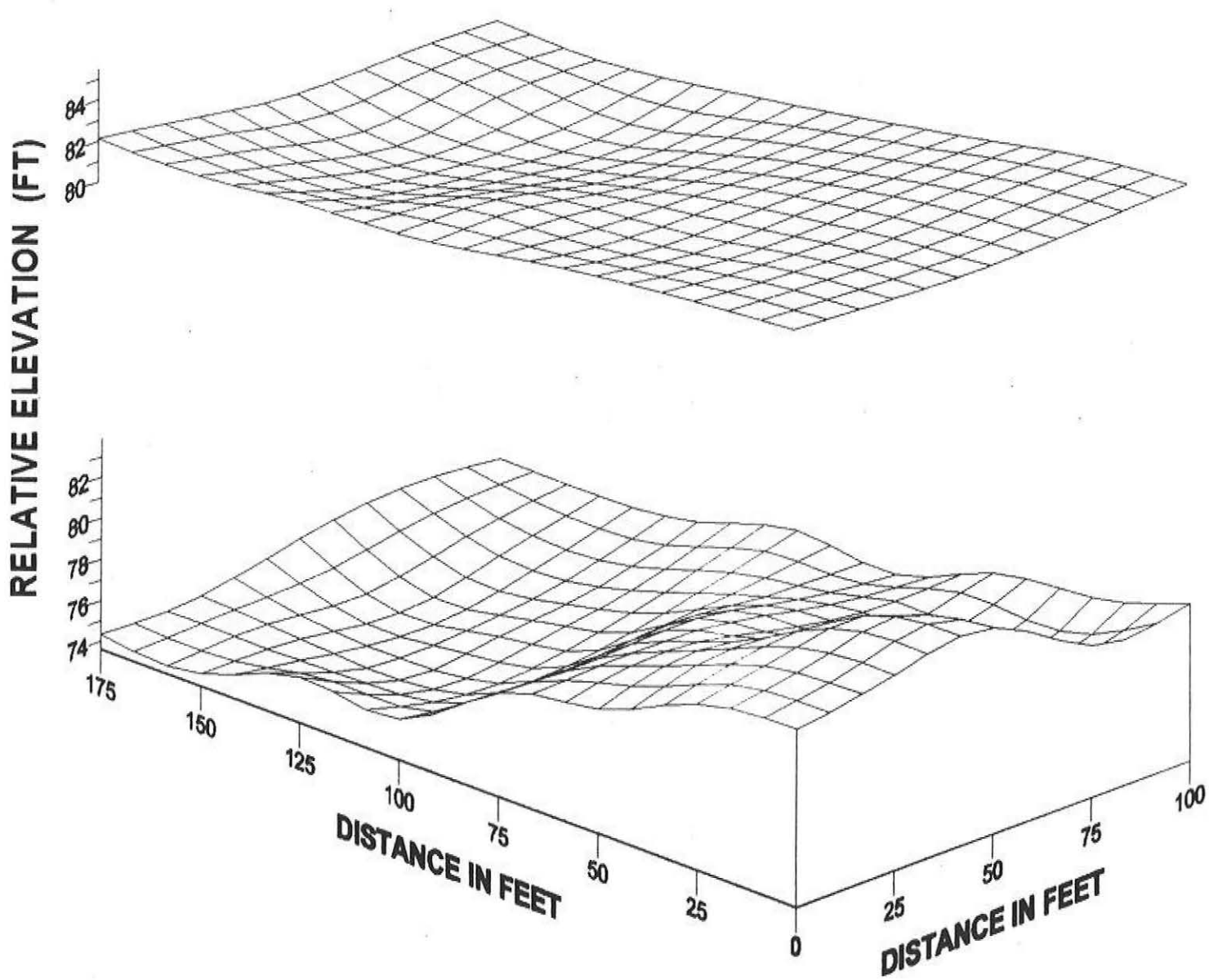

THICKNESS OF SANDS

ESTIMATED WITH EM

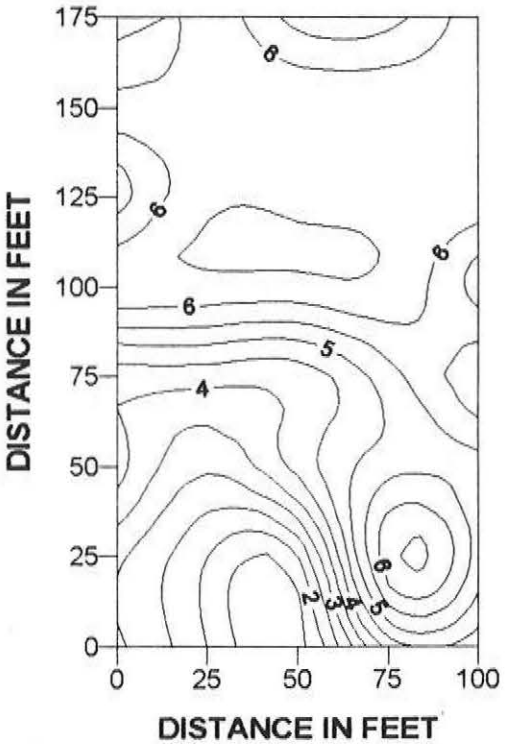
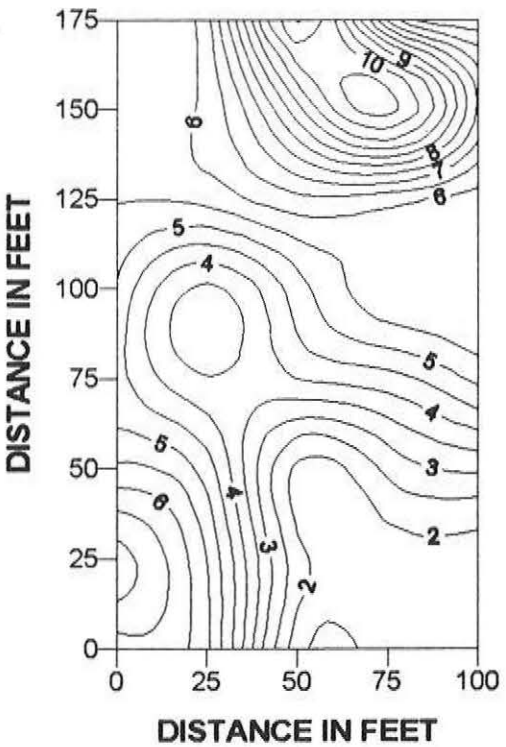
ESTIMATED WITH GPR